Project Description – Project Proposals

Florian Kummer, Darmstadt

Highly accurate numerical simulation of wetting, dewetting and fluid-splitting phenomena between elastic surfaces

---

Project Description

The purpose of this project is to provide highly accurate numerical simulations, based on the discontinuous Galerkin (DG) method, for the simulation of the interaction of liquids with flexible substrates. This includes especially simulation of the wetting behavior of the flexible solid.
Such processes have many technically relevant applications, one of them being e.g. flexographic printing, where water-based ink is applied onto an elastic surface and from there onto the subject to print.
The complex interaction between three phases (gas/liquid/flexible solid) as well as the dynamics of the three-phase contact line require numerical methods, which are able to represent the underlying mathematical models with high precision in order to gain exact knowledge about the hydrodynamic effects. The models, e.g. for contact line dynamics, usually contain singular terms, e.g. forces which are only active on the 2D interface or the 1D contact line.
In the present project, the high precision required to capture the singular behavior is guaranteed through a cut-cell DG (also called extended or unfitted DG) method where singular forces can be implemented without regularization, i.e. `smearing' of jumps and Dirac-deltas.

1 State of the art and preliminary work

Problem Statement

The physical model used in this project is a three-phase system containing gas, a viscous fluid and a deformable solid. The velocity $\boldsymbol{u}(t,\boldsymbol{x})$ and pressure $p(t,\boldsymbol{x})$ in the bulk phases of gas and liquid are determined by the incompressible Navier-Stokes equation

$$\partial_t(\rho\boldsymbol{u}) + \operatorname{div}(\rho\boldsymbol{u}\otimes\boldsymbol{u}) + \nabla p = \operatorname{div}(\mu\,\boldsymbol{D}(\boldsymbol{u})), \tag{1}$$

$$\operatorname{div}(\boldsymbol{u}) = 0 \tag{2}$$

with piece-wise constant density ρ and viscosity μ, and tensor $\boldsymbol{D}(\boldsymbol{u}) \coloneqq (\nabla\boldsymbol{u} + \nabla\boldsymbol{u}^{\mathrm{T}})$ while the displacement $\hat{\boldsymbol{w}}(t,\boldsymbol{\xi})$ of the solid phase is, in the most simple case, modeled by the equations

$$\partial_{tt}(\rho\hat{\boldsymbol{w}}) = \operatorname{div}_{\boldsymbol{\xi}}(\hat{\boldsymbol{T}}_S(\hat{\boldsymbol{w}})), \tag{3}$$

with solid stress tensor $\hat{\boldsymbol{T}}_S(\hat{\boldsymbol{w}})$. In the simplest case of isotropic linear elasticity, $\hat{\boldsymbol{T}}_S$ can be written using Lamé constants, i.e.

$$\hat{\boldsymbol{T}}_S(\hat{\boldsymbol{w}}) = \lambda_S\operatorname{div}_{\boldsymbol{\xi}}(\hat{\boldsymbol{w}})\boldsymbol{I} + \mu_S\boldsymbol{D}(\hat{\boldsymbol{w}}). \tag{4}$$

Note that, while the fluid system is noted in a Eulerian frame, the solid system is defined in a Lagrangian framework, as noted by the `hat'-notation; e.g. $\hat{\boldsymbol{w}}$; a superscript $\boldsymbol{\xi}$ denotes derivatives with respect to solid coordinates, e.g. $\operatorname{div}_{\boldsymbol{\xi}}$.

Fluid-Solid coupling: at the fluid/solid interface the coupling conditions are

$$\boldsymbol{u} = \partial_t\boldsymbol{w}, \tag{5}$$

$$(-p\boldsymbol{I} + \mu\, \boldsymbol{D}(\boldsymbol{u})) \cdot \boldsymbol{n} = \boldsymbol{T}_S. \tag{6}$$

Note that the coupling stated above is defined in the Eulerian frame. Hence, an additional transformation relation between Lagrangian properties $\widehat{\boldsymbol{w}}$ and $\widehat{\boldsymbol{T}}_S$ and Eulerian properties $\boldsymbol{w}$ and $\boldsymbol{T}_S$ is required

Liquid-Gas-coupling: The fluid/gas interface $\mathcal{J}$ is assumed to be material and allows no tangential slip, furthermore, one usually assumes continuity of stresses, i.e.

$$[\![\boldsymbol{I}p - \mu\boldsymbol{D}(\boldsymbol{u})]\!] \cdot \boldsymbol{n}_{\mathcal{J}} = \nabla_{\mathcal{J}}\sigma - \ \sigma\, \mathrm{div}_{\mathcal{J}}(\boldsymbol{n}_{\mathcal{J}})\boldsymbol{n}_{\mathcal{J}}, \tag{7}$$

$$[\![\boldsymbol{u}]\!] = 0 \tag{8}$$

where $\boldsymbol{n}_{\mathcal{J}}$ denotes the interface normal, $\nabla_{\mathcal{J}}$ and $\mathrm{div}_{\mathcal{J}}$ denote surface gradient and divergence and σ denotes surface tension, which may be non-constant, e.g. depends on the presence of surfactants or non-uniform temperature.

Contact line: At the three-phase contact line, the thermodynamic consistent modelling is still under scientific debate. A common choice is a line force which incorporates the uncompensated Young stress and optionally a dissipative term. However, the general modelling of contact lines is a matter of active research.

Discontinuous Galerkin methods

In this project, a Discontinuous Galerkin (DG) method is used to solve, resp. simulate the mathematical model described above. Its origins can be tracked back to the work of Reed and Hill [1]. However, DG methods gained attention e.g. through the works of Cockburn [2] or Arnold [3], just to mention two.

The general idea is to represent any field $u(\boldsymbol{x})$, e.g. velocity or pressure, by a weighted sum over a set of basis polynomials $\phi_{j,n}$

$$u(\boldsymbol{x}) \approx u_h(\boldsymbol{x}) = \sum_{j,n} u_{j,n}\phi_{j,n}(\boldsymbol{x})\,, \tag{9}$$

on the computational mesh $\mathfrak{K}_h = \left(K_1, \dots, K_J\right)$, consisting of cells K_j, with a characteristic mesh width h.

Such an approximation provides high-order convergence properties, e.g. for the approximation of a scalar u, one observes the error convergence

$$\|u - u_h\|_{L^2} \leq Ch^{k+1}, \tag{10}$$

where k is the polynomial degree of the interpolation. This relation, however, requires that the interpolant u is sufficiently smooth, i.e. k times continuously differentiable.

Extended discontinuous and continuous Galerkin methods.

The multiphase problem stated above typically has solutions of low regularity at the gas/liquid interface and at the contact line, due to jumps in density and viscosity and because of surface tension effects. The velocity field features a kink, i.e. the velocity gradient is discontinuous and the pressure features a jump. Under such circumstances, high order methods like DG usually degenerate to low order convergence or even become unstable. One overcomes this issue by adapting the approximation space to the fluid interface.

This idea of adapting a finite element method (FEM) to allow jumps in parameters can be traced back to the 1970s, where Poisson problems with a jump in the diffusion parameter along a smooth interface were investigated by Babuška [4] as well as by Barrett and Elliott [5]. A very prominent idea, called the extended finite element method (XFEM), was presented by Moës et al. [6] to simulate cracking phenomena in solid mechanics. Those ideas were extended to time-dependent problems by Chessa and Belytschko [7].

The first XFEM for two-phase flows was presented by Groß and Reusken [8] [9]. With the so-called intrinsic XFEM presented by Fries [10], it became possible to represent also kinks in the velocity field. This work was later extended by Cheng and Fries [11] and further by Sauerland and

Fries [12]. The first extended DG (XDG) method (also called unfitted DG or cut-cell DG) was presented by Bastian and Engwer [13] in order to model flows in porous media. Later, those approaches were extended to multi-phase flows by Heimann et al. [14].
One strength XFEM/XDG is that it allows to simulate any kind of dynamic interface or surface that would be difficult to mesh using a conventional mesh generator, especially if also topology changes occur (e.g. merging of droplets, detachment from surfaces). This feature makes XFEM/XDG methods very interesting for the simulation of two-phase flows. The position of the fluid interface can be described as the (zero-) level-set of a scalar field $\varphi(t, \boldsymbol{x})$, which is subject to the evolution equation

$$\partial_t \varphi + \nabla \varphi \cdot \boldsymbol{u} = 0. \tag{11}$$

Note that the level-set itself is typically discretized by a standard, non-extended FEM/DG method while XFEM/XDG is used for the discretization of fluid properties.

Fluid-structure interaction
Solutions to fluid-structure interaction (FSI) problems require the coupling of two very different solvers, i.e. it consists of a hydromechanics solver for the Navier-Stokes equations (1-2) and a second solver for the solid mechanics equations (3-4). Since there is a large number of software packages available for both problems, it is attractive to couple already existing solvers. A usual approach would e.g. be to transform displacements, velocities and accelerations into the fluid domain, acting as Dirichlet conditions to the flow solver. For the structural solver, fluid stresses are transformed into the solid domain and applied as Neumann boundary conditions.
A common approach is to call each solver once per time-step and exchange data according to the Dirichlet-Neumann coupling conditions (5-6). This is referred to as a loosely coupled scheme. Their main advantages are modularity and a simple implementation. However, in a work of Causin et. al. [15] it was proven that for certain combinations of physical and geometric parameters Dirichlet-Neumann loosely coupled schemes are unconditionally unstable due to the so-called added-mass effect. Yet, since loose coupling is very attractive in terms of implementation, there is an extensive amount of works which analyze the stability for a specific problem and propose various solutions to overcome stability problems, see e.g. the works of Lukáčová-Medvid'ová et. al. [16], Bazilevs et al. [17] or Beirão da Veiga [18].
However, loosely coupled schemes can be converted into strongly coupled ones, even if both solvers are spread out between two software packages. The simplest realization is a fix-point method, which iterates between both solvers; however, such methods are prone to slow convergence behavior. There is, however the option to use e.g. a Newton method to improve convergence, as e.g. demonstrated by Matthies and Steindorf [19], where an iterative, Jacobi-free Newton method is used to solve the strongly coupled system. The convergence can be further improved by appropriate block-preconditioning techniques [20], where each block correspond to one of the two solvers.
Most of the above-mentioned works employ an ALE formulation ("moving meshes") in order to model the change of the fluid domain over time. However, there is also the option to represent the fluid/solid boundary by an XFEM approach. Such an approach was used e.g. in the work of Alauzet et. al. [21] to simulate interaction of flow with a thin membrane.
A very recent work in the domain of XFEM FSI by Antonietti et. al. [22] demonstrates the coupling of a three-dimensional solid structure to a flow by a Nietsche method, i.e. using penalty formulations. Both of these works fall into the category of strongly coupled, monolithic methods.

Modelling of contact line problems
The numerical simulation of three-phase contact lines, resp. wetting and de-wetting processes on surfaces has long been an object of active research, however, predictive numerical methods, which manage without configuration-dependent parameters, are only applicable for very special problems see e.g. the works of Sprittels and Shikhmurzaev [23] or Legendre and Maglio [24]. This fact can be traced back to a manifold of mutually influencing problems, which occur in the area of the moving contact line in addition to the classical challenges for simulations of multiphase flows of immiscible fluids. The requirements to the grid resolution in the close vicinity of the moving contact line are a big challenge for the performance of direct numerical simulations of such flows.

Two-phase and contact line simulations at Chair of Fluid Dynamics

Numerical Integration in cut cells: Research in the field of XDG methods for two phase flow simulations has been a cornerstone at the Chair of Fluid Dynamics over the last couple of years. An important prerequisite for the implementation of high order XDG methods is the ability to perform highly accurate numerical integration in cells cut by the level set, which has been addressed in the works of Müller et. al. [E1] [E2], where the so-called Hierarchical Moment Fitting (HMF) approach was developed.

Based upon these integration techniques, we developed a solver for the simulation of two-phase flow, see Kummer [E3]. A major part of this work is devoted to the solution of numerical problems in XDG methods related to small cut cells, i.e. when the interface cuts a cell very close to an edge or corner of the background cell. We developed a cell agglomeration technique which successfully overcomes these issues. A very critical part in the simulation of multiphase flows is the evaluation of the curvature $\kappa = \mathrm{div}_{\mathcal{J}}(\boldsymbol{n}_{\mathcal{J}}) = \mathrm{div}_{\mathcal{J}}(\nabla\varphi/|\nabla\varphi|)$, which is proportional to the force at the fluid interface, see Eq. 7, since it is a nonlinear function of first and second derivatives. In a separate work [E4], we developed patch-recovery filters in order to stabilize the curvature evaluation.

Level-Set methods: In order to solve flow problems with moving interfaces, it is commonly known that the level-set field $\varphi(t,\boldsymbol{x})$ has to be re-initialized from time to time, e.g. every 10 to 20 time-steps due to the requirement of numerical stability. Re-initialization is the process of replacing $\varphi(t,\boldsymbol{x})$ with another field $\varphi^*(t,\boldsymbol{x})$ that has the same zero-set and sign, but fulfills the signed-distance property, resp. the Eikonal equation

$$|\nabla\varphi^*| = 1. \tag{12}$$

In Utz et. al. [E5] we presented novel re-initialization approaches for high-order DG level-set methods based on an energy minimization approach which converges to vanishing viscosity solutions without additional king-detection techniques that are required e.g. in hyperbolic reinitialization techniques, see e.g. Karakus et. al. [25].

A fundamental problem in the coupling of the flow solver to the level-set in Eq. (11) is that the velocity $\boldsymbol{u}$ is a member of the XDG space, while the level-set field φ itself is a member of the non-extended DG space. Per construction, $\boldsymbol{u}$ contains a singularity at the zero-level-set itself. Therefore, a large local projection error at the interface is introduced, which is especially unfavorable since the vicinity of the zero-set is the only region where the values of the level-set field are of interest. One possible solution is to use an velocity extension: In Eq. (11), the flow velocity $\boldsymbol{u}$ is replaced by a velocity $\boldsymbol{u}^*$ that fulfills three properties: It is equal to $\boldsymbol{u}$ at the interface itself, it is constant in normal direction (i.e. fulfills $\nabla\varphi \cdot \boldsymbol{u}^* = 0$) and it is continuous, i.e. has no kink at the interface. In the context of DG methods, such a level-set evolution algorithm was developed by Utz et. al. [E6]. Additionally, the use of a velocity extension reduces the amount of required re-initializations. Since the extension problem is linear, it is also cheaper to solve than the re-initialization problem.

Time discretization for moving domains: For problems with static domains, space and time discretization can be treated independently, i.e. a DG approach in space can be formally combined with any time integrator, e.g. a Runge-Kutta method. Depending on the equation to be solved, as well as the ratio of spatial and temporal resolution, either the spatial or the temporal error is dominant.

In a study of Kummer et. al. [E7], the application of conventional time integrators (Runge Kutta, BDF) to problems with moving interfaces was investigated. Two fundamentally different approaches, referred to as ‘splitting’ and ‘moving interface’, were found for this purpose, the latter being clearly superior. In particular, we showed that for problems with moving interfaces, the spatial and temporal discretization can no longer be considered independently of each other: it was shown that the numerical error can increase with spatial refinement, if the time is not refined to the same extent.

Flows with moving domains: Considering the above mentioned time discretizations for moving domains, several simulations of rigid body movement have been investigated by Krause and Kummer [E8]. For this, an explicit coupling approach between the Navier-Stokes Equations and the Newton-Euler Equations of motion was used. The effects of the fluid onto the rigid bodies are

considered by using the integration technique on cut cells for hydrodynamic force and torque. The ability of the method was shown for arbitrary motion of one circular body immersed in the fluid domain. Comparing with literature in the field, large number of degrees of freedom could be saved with our approach though still reaching the same computational accuracy.
Further, the method is currently extended to rigid body motions with arbitrary shape and a particle-particle and particle-wall collision model based on the conservation of momentum and kinetic energy. An extension to three dimensional flows is considered next and the basic concept was already proven to work for simple flows, e.g. around a sphere.

Contact line modelling: Recently, within the context of the Collaborative Research Centre 1194, the our XDG-based two-phase flow solver has been upgraded to support three-phase contact lines. Presently, the solid phase is assumed rigid, i.e. no simulation is necessary. Due to the extended Galerkin formulation, the contact line model can be implemented in a very natural way. The currently implemented standard model incorporates a generalized Navier-Slip boundary condition at the solid/liquid and the solid/gas boundary and an additional force at the contract line, which is given as

$$\boldsymbol{f}_L = \big(\beta_L(\boldsymbol{u}\cdot\boldsymbol{t}) - \sigma(\cos(\theta_e) - \cos(\theta))\big)\boldsymbol{t}, \tag{13}$$

where β_L is a line dissipation coefficient, $\boldsymbol{t}$ the tangent on the solid wall and normal onto the contact line, θ_e the static contact angle and θ the actual contact angle. Preliminary results are shown in **Figure 1** and **Figure 2**. Currently, the implementation is extended towards more complex contact line models which e.g. support contact angle hysteresis.

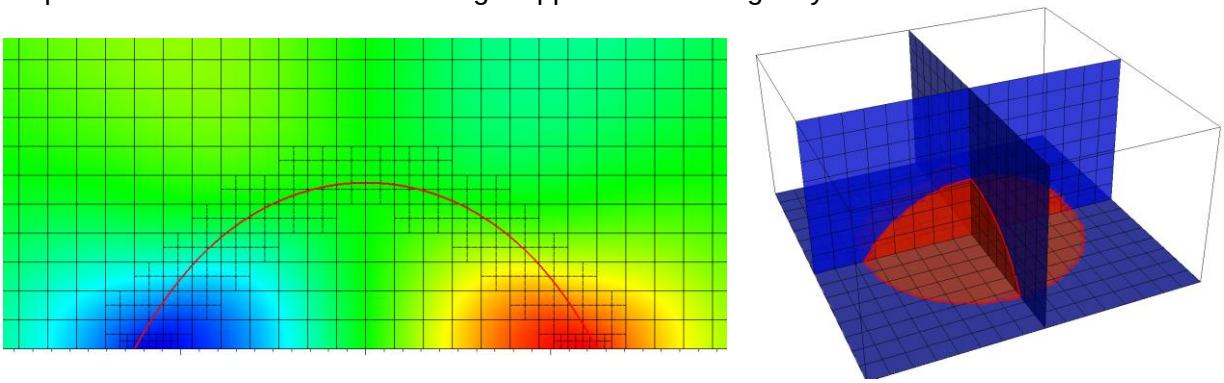

Figure 1: *XDG-Simulation of droplet sitting on a simple surface, in 2D as well as in 3D. As visible on the left, the implementation also supports adaptive mesh refinement.*

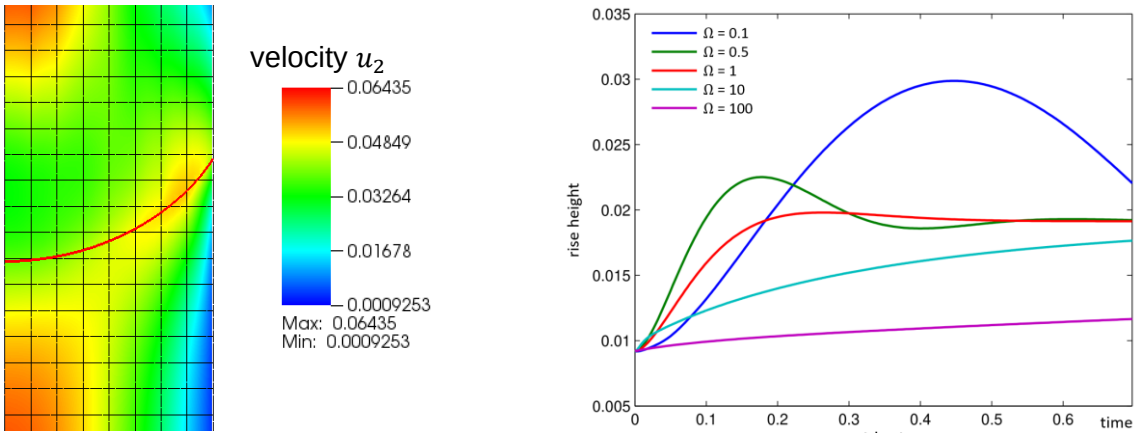

Figure 2: *XDG Simulation of capillary rise; showing the rise height over time for various values of the dimensionless variable* $\Omega = \sqrt{(9\sigma\cos(\theta_e)\,\mu^2)/(\rho^3 g^2 R^5)}$

Code development: All methods and developments mentioned above have been combined in a single, unique software package, which is referred to as the BoSSS (Bounded Support Spectral Solver) code. It is a flexible software framework for the development of XDG schemes and has

been applied to a broad range of problems; this includes further topics not discussed here, e.g. compressible and reactive flows.
Over almost ten years of development, BoSSS became a versatile toolbox for the design of new DG and XDG methods, due to a unique combination of features. Its highlights are:

- Support for problems with dynamic interfaces: By combining XDG and level-set algorithms, BoSSS becomes capable of handling a broad range of dynamic interfaces or boundaries [E4, E8, E9]
- Rapid prototyping capability: New models resp. equations can be added in a notation that is close to the usual presentation of DG methods in textbooks, with low development effort. Technical issues, e.g. the handling of the numerical mesh, are provided by the software library, as e.g. demonstrated in [E10].
- Suitability for High Performance Computing (HPC): All production algorithms in BoSSS are implemented MPI parallel. Furthermore, BoSSS provides instrumentation output in order to analyze and optimize parallel scaling as well as node-level performance.
- Adaptive mesh refinement: multiphase flow problems typically show a huge variety of length scales, e.g. the surface radius of a rising bubble covers several magnitudes. Since the location of the respective features changes dynamically, mesh adaptation during runtime is essential.
- Dynamic load balancing: allows re-distribution of the computational mesh when a level-set enters or leaves the domain of the respective MPI processor.
- Sophisticated workflow and data management facilities: In order or organize and analyze e.g. large parameter studies (simulation setup, storing results and perform post-processing), database-centric workflow tools were developed.

Up to date, BoSSS has been used for 9 completed PhD theses and is used in 8 active PhD projects series of PhD thesis as well as DFG-funded projects, including:

- Collaborative Research Centre 568 (3rd funding period)
- Priority Programme 1506 (two funding periods)
- Collaborative Research Center 146 (TRR 146, 2nd period, ongoing) in cooperation with the Numerical Mathematics group at Johannes Gutenberg University Mainz
- Collaborative Research Center 1194 (1st funding period, ongoing)

Technical Applications

Flexography: The technical application which is the motivation for this proposal is flexographic printing. Here, a flexible printing plate is used to transfer liquid (e.g. ink) to a substrate surface (e.g. paper) – for a comprehensive overview, see e.g. the work of Ganz et. al. [26]. The main advantage of flexographic printing is that environment-friendly, water-based ink could be used, instead of ink based on mineral oil, which is required for offset printing.
In physical terms, this type of printing is characterized by the wetting and de-wetting of elastic surfaces. A critical element in the process is the ink separation at the meniscus at the outgoing edge of the nip. Close to this point, one observes several flow instabilities, e.g. the occurrence of air fingers which penetrate the meniscus. These unwanted effects are responsible for printing imperfections, e.g. for viscous fingering. Physical observations hint that the flexible printing plate and the fluid form some kind of self-regulating system. It is further observed, that with higher printing velocities, the issue of viscous fingering is improved. The flexible printing plate also seems to help to stabilize the process with respect to geometric imperfections, resulting e.g. form manufacturing tolerances.
A better understanding of the interplay between elastic and viscous forces, surface tension and de-wetting is required for the improvement of flexographic printing procedures.

1.1 Project-related publications

1.1.1 Articles published by outlets with scientific quality assurance, book publications, and works accepted for publication but not yet published.

- [E1] B. Müller, F. Kummer, M. Oberlack and Y. Wang, “Simple multidimensional integration of discontinuous functions with application to level set methods”, *Int. J. Numer. Methods Eng.*, vol. 92, no. 7, pp. 637–651, 2012.
- [E2] B. Müller, F. Kummer and M. Oberlack, „Highly accurate surface and volume integration on implicit domains by means of moment-fitting”, *Int. J. Numer. Methods Eng.*, vol. 96, no. 8, pp. 512–528, 2013.
- [E3] F. Kummer, “Extended discontinuous Galerkin methods for two-phase flows: the spatial discretization”, *Int. J. Numer. Methods Eng.*, vol. 109, no. 2, pp. 259–289, 2017.
- [E4] F. Kummer and T. Warburton, “Patch-recovery filters for curvature in discontinuous Galerkin – based level-set methods”, *Comm. Comp. Phys.*, vol. 19, no. 02, pp 329–353, 2016.
- [E5] T. Utz, F. Kummer and M. Oberlack: “Interface-preserving level-set reinitialization for DG-FEM”, *Int. J. Numer. Methods Fluids*, vol. 84, no. 4, pp. 183–198, 2017.
- [E6] T. Utz and F. Kummer, “A high-order discontinuous Galerkin method for extension problems”, *Int. J. Numer. Methods Fluids*, vol. 86, no. 8, pp. 509–518, 2017.
- [E7] F. Kummer, B. Müller and T. Utz, “Time integration for extended discontinuous Galerkin methods with moving domains”, *Int. J. Numer. Methods Eng.*, vol. 113, no. 5, pp. 767–788, 2017.
- [E8] D. Krause and F. Kummer, “An incompressible immersed boundary solver for moving body flows using a cut cell discontinuous Galerkin method”, *Computers & Fluids*, vol. 153, pp. 118–129, 2017.
- [E9] B. Müller, S. Krämer-Eis, F. Kummer and M. Oberlack, “A high-order discontinuous Galerkin method for compressible flows with immersed boundaries *Int. J. Numer. Methods Eng.*, vol. 110, no. 1, pp. 3–30, 2017.
- [E10] B. Klein, B. Müller, F. Kummer and M. Oberlack, “A high-order discontinuous Galerkin solver for low-Mach number flows”, ”, *Int. J. Numer. Methods Fluids*, vol. 81, no. 8, pp. 489–520, 2016.

1.1.2 Other publications

none

1.1.3 Patents

none

2 Objectives and work programme

2.1 Anticipated total duration of the project

36 Months, starting at 1st of October, 2019.
(first funding period of Priority Programme with possible extension to second period)

2.2 Objectives

We provide a highly accurate numerical toolbox for the simulation of three-phase systems comprising of a flexible solid, as well as a liquid and a gaseous phase.
The principal experiment for this project is the behavior of a three-phase contact line on a flexible substrate as well as the impact and wetting of a droplet on such a surface.

The application perspective for this project, within the scope of the Priority Programme, is, but not limited to, flexographic printing. In order to better understand the appearance of printing

imperfections caused by viscous fingering, numerical simulations will provide quantities, which are difficult to obtain through measurements, e.g. flow profiles within the nip. Furthermore, parameter studies will be used to verify scaling laws predicted by theory. Simulations also allow to study variation of parameters like viscosity, which are difficult to change in the experiment and thus, to provide optimized parameters which avoid printing imperfections as far as possible.
In addition to flexographic printing, the numerical toolbox will be further useful for a broad range of applications within the Priority Programme.

Test setups:
Together with cooperation partners (see also section 2.8), we agreed on four different configurations to investigate different aspects of the physical problem. The first two experiments (**Figure 3** and **Figure 4**), in cooperation with K. Harth (University of Twente), investigate basic principles, i.e. the movement of the contact line and the impact and wetting behavior on a flexible surface. The third and fourth experiment (**Figure 5** and **Figure 6**), in cooperation with E. Dörsam (TU Darmstadt, Printing Science Technology) investigate technical applications of those principles.

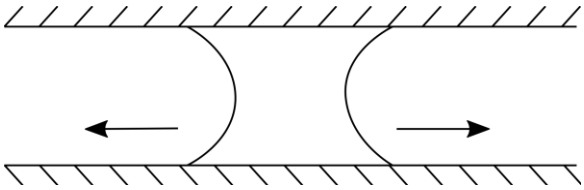

Figure 3: *Elementary experiment „liquid bridge“: a liquid bridge is placed in between two plates. Via the plate movement, one is able to control the wetting patch.*

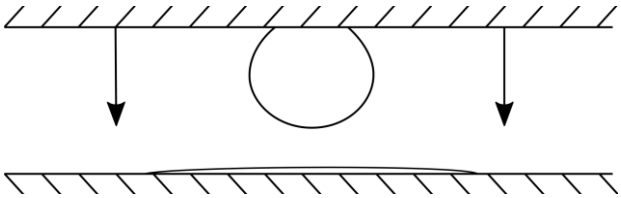

Figure 4: *Elementary experiment „Droplet impact“: a drop attached to a solid surface on the top is lowered at a controlled rate onto a flexible substrate until contact is made.*

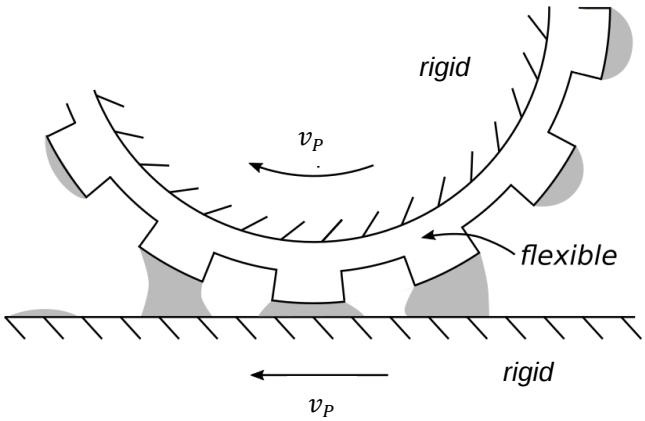

Figure 5: *Printing setup „Flexible Roller“: The flexible printing plate is mounted on the printing cylinder. Ink is already applied to the printing form, resting as droplets or films which are pinned at the edges of the elevated part of the printing plate. These finite films are then brought in contact with a rigid surface, moving with the same velocity as the printing form, to which the ink is transferred. On the outgoing edge of the nip, the ink is separated and hydrodynamic instabilities (fingering) can be observed, as air penetrates into the liquid interface.*

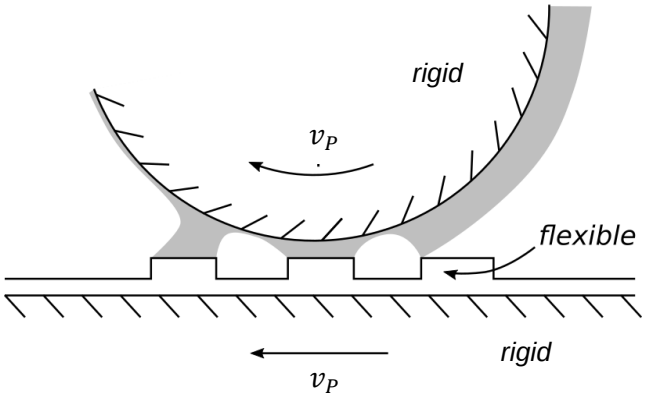

Figure 6: *Printing setup „Flexible Substrate“: the printing roller is covered with a continuous film of ink. The flexible printing plate is mounted on a moving shuttle. Note that there is no direct contact between the printing plate and the roller. On the outgoing edge of the nip, the ink is separated, which and hydrodynamic instabilities (fingering) can be observed, as air penetrates into the liquid interface.*

Objectives for *elementary experiments*

Liquid bridge:

The “liquid bridge” configuration (**Figure 3**) is a very attractive experiment for the **validation** of the basic principles of the numerical simulation, mainly because it does not change topology during the experiment, with the exception of the case where the liquid bridge breaks up.

For the comparison of simulation and experiment, we focus on the following integral properties:

- **position and velocity of contact line**, as well as **instantaneous contact angle**
- the **static deformation of the flexible substrate**

Furthermore, the liquid bridge configuration, by moving the surfaces apart, can trigger **a ligament breakup** which can be qualitatively compared to the simulation.

Droplet impact:

The main question which should be answered by the numerical reproduction of the “droplet impact” (**Figure 4**) setting is whether the standard model, based the contact line force balance, as in Eq. (13), is capable of correct reproduction of the impact event and the initial wetting.

Note that the exact physical effects for the initial wetting, resp. the droplet contact are still not very well understood. It seems plausible that, on impact, the droplet first deforms and a microscopic air film develops. For the initial wetting, i.e. the bridging of the microscopic air film, Van-Der-Waals forces as well as surface contamination may play a role.

Certainly, all these effect are not present in the numeric, at least not in the standard model, represented by Eq. (13) (augmented with contact line hysteresis). The air film is so thin that it may not be possible to resolve it numerically.

Note that, without the introduction of additional models into the simulation, the initial wetting/bridging of the film is an artifact; Numerically, the fluid and the solid interface cross over in between two time steps. After the topology has changed the contact line model becomes active; since the contact angle, initially, is large, a strong line force will be induced at the contact line.

The question is: how does the **replacement of effects which are beyond continuum physics by numerical artifacts compromises the overall validity** of the simulation results?

For both setups, there are several properties which are difficult to measure in experiments, but which are of high interest for the cooperation partners:

- **flow profile** in the droplet with **temporally synchronized deformation data** of the substrate
- **substrate deformation** together with the **stress profile**
- general information on internal fields which are not visible for measurements

Objectives for *printing setups*

According to cooperation partners, the following properties and characteristics are of particular interest for printing:

- The shape of the elastic deformation of the substrate in the nip as well as the position of the wetting border.
- The flow and pressure profile in the nip
- An first indication of whether pressure peaks occur in the nip, which can lead to cavitation
- Insights into the self-stabilizing mechanism of the flexographic setup. Therefore, the flexible substrate will be computationally replaced by discrete series of 1D spring/damper/mass systems.

The (unwanted) occurrence of viscous fingering is certainly a three-dimensional effect; thus, it requires fully developed 3D simulations.
The following integral measures of the simulation should be compared to the experiment:

- The dynamic shape of the wetting border: Since it is influenced by an instability, the exact shape of the contact line is the result of a stochastic process; however, one can compare several integral properties, e.g. its position averaged over time and in span-wise direction. Furthermore, a **Fourier series in space and time** can represent the **shape of the wetting border**. Thus, one can compare **wavelengths** as well as **amplitudes** to the experiment.
- The formation of viscous fingers on the outgoing side of the nip. Integral properties of those, e.g. the **statistical distribution of width and length of fingers** will be compared to experiments.

Moreover, the purpose of numerical simulation is not limited to confirming the experiment. There are several properties which are difficult to measure in experiments, but which are of high interest for the cooperation partners:

- The qualitative **flow profile** in the nip, and what shear rates can be expected
- The **pressure profile** in the nip: According to rough estimates, the occurrence of cavitation events in the nip appears plausible, but is not yet verified nor falsified by experiments. Obviously, the incompressible fluid model in this project cannot capture cavitation. However, there should be a good indication of the existence of pressure peaks that can cause cavitation.
- A parameter study will determine the threshold value for the printing speed above which the **capillary forces dominate the viscous forces**.
- The identification of **parameter ranges which avoid printing imperfections**.

2.3 Work programme incl. proposed research methods

Methodology: Fluid-Structure coupling using level-sets
In addition to the liquid/gas interface $\mathcal{I}$, realized via the level-set-field φ, this project requires the numerical representation of a second interface between the fluids and the flexible solid. For the implementation of this second interface two options are at hand:

- An arbitrary Lagrangian-Eulerian (ALE) approach: this requires the implementation of moving meshes the respective ALE terms into the multiphase flow solver and the level-set solver.
- A level-set approach: a second level-set $\varphi_2(t, \boldsymbol{x})$ is used to describe either the solid boundary in the sense of a (conservative) Immersed Boundary Method (IBM) resp. the additional fluid interface. It is important to note that the XDG implementation in BoSSS is already capable of tracking more than two phases; what is currently missing is numerical integration for cells that are cut by two level-sets, which is not possible with the current HMF approach. However, a further integration technique is implemented based on a simple adaptive subdivision – currently rarely used in favor of the HMF approach – which could easily be extended to several level-sets.

We consider the second option to be easier to implement. The level-set approach is also more versatile than the ALE method for the particular simulation objectives of this project. E.g., the level-set approach also would give us the opportunity to extend the formulation to systems with multiple fluids (e.g. systems containing air, water and oil) in the second funding period. Based on the current state of knowledge, it therefore seems justified to focus exclusively on the level-set approach.

Conversion of Lagrangian displacement into a level-set: We propose to following method to transfer the Lagrangian displacement vector $\widehat{\boldsymbol{w}}$ into a level-set field φ_2 and the corresponding level-set $\mathcal{I}_2(t) = \{\boldsymbol{x};\ \varphi_2(t,\boldsymbol{x}) = 0\}$, which describes the boundary between solid and fluid, in the Eulerian frame.
Let $\widehat{\Omega}_S$ be the domain of the completely relaxed solid body, i.e. the domain on which the displacement vector $\widehat{\boldsymbol{w}}$ and the elasticity equation (3) are defined. Further, let $\Omega_S(t)$ be the solid domain in the Eulerian frame, at time t, whose deformable boundary should be described by the level-set φ_2. By using the Lagrangian map,

$$\mathcal{L}: \widehat{\Omega}_S \longrightarrow \mathbb{R}^D,\ \ \boldsymbol{\xi} \mapsto \boldsymbol{\xi} + \widehat{\boldsymbol{w}}(\boldsymbol{\xi}) \tag{14}$$

one could notate $\Omega_S(t)$ as the image of $\widehat{\Omega}_S$, i.e. $\Omega_S(t) = \mathcal{L}(\widehat{\Omega}_S)$.
It is assumed that the initial displacement is identical to zero, i.e. $\Omega_S(0) = \widehat{\Omega}_S$ and $\mathcal{I}_2(0) \subseteq \partial\widehat{\Omega}_S$. For times $t > 0$, we track φ_2, resp. $\mathcal{I}_2$, by a level-set evolution equation analogously to equation (11) presented above; therefore, an evolution velocity $\boldsymbol{u}_2$ is required.
At the zero set itself, the time derivative of the displacement, $\partial_t\widehat{\boldsymbol{w}}$, defines an evolution speed of the solid/fluid boundary. Since $\partial_t\widehat{\boldsymbol{w}}$ is unknown outside of the domain $\Omega_S(t)$, we construct an evolution velocity $\boldsymbol{u}_2$ by solving the PDE

$$\nabla\varphi_2 \cdot \boldsymbol{u}_2 = 0, \tag{15}$$

$$\boldsymbol{u}_2 = \partial_t\widehat{\boldsymbol{w}} \quad \text{on} \quad \{\boldsymbol{x}; \varphi_2(t,\boldsymbol{x}) = 0\}, \tag{16}$$

as described in section 1, resp. in Utz et. al. [E5]. Then, φ_2 can be updated using the constructed velocity $\boldsymbol{u}_2$. Note that the implementation of the boundary condition (16) requires the inversion of $\mathcal{L}$ at the interface $\mathcal{I}_2$, since (16) it is implemented in a weak form in the Eulerian frame.
Obviously, the procedure described above is prone to the accumulation of numerical error, i.e. in each time-step the difference between the zero-level-set $\mathcal{I}_2$ and $\widehat{\boldsymbol{w}}$ may grow. Therefore, a correction procedure which re-aligns $\mathcal{I}_2$ with $\widehat{\boldsymbol{w}}$ be necessary, at least after a finite number of time-steps.
Since φ_2 is signed-distance, the value $\varphi_2(t, \mathcal{L}(t,\boldsymbol{\xi}))$, for some $\boldsymbol{\xi} \in \partial\widehat{\Omega}_S$, gives an approximation of the distance between the actual and the supposed position of $\mathcal{I}_2$. In the next time-step, this information can be used to add a correction velocity in the boundary condition (16).

Coupling of structural solver: As outlined in the works of Matthies and Steindorf [19], we intent to use a non-monolithic approach for the FSI. Instead of developing a own structural solver we intend to use an external package such as e.g. COMSOL, which can be controlled via a Java-based application program interface (API).
The advantages of such an approach are two-fold: first, it allows us to skip the development time required for a structural solver. Time is a crucial factor in the setup of collaboration work-packages. Second, packages like COMSOL usually provide an extensive library of different material models, including not only linear elasticity but also viscoelastic material laws.
The first development step is thus the implementation of loose coupling, i.e. splitting where both, flow and structure solver are called once per time-step. Via the interface $\mathcal{J}_2$ which is constructed from the displacement vector field, a structural solver imposes Dirichlet boundary conditions onto the flow solver. Vice-versa, via the interface condition (6), the stress from the fluid at the interface is transferred to the structural solver, acting as a Neumann boundary condition. Therefore, the Cauchy stress tensor $\boldsymbol{T}_S$ hast to be converted into the Piola-Kirchhoff tensor $\widehat{\boldsymbol{T}}_S$, which are related via the deformation gradient $\boldsymbol{F}$ by the transformation

$$\boldsymbol{T}_S = \boldsymbol{F}^{-1} \cdot \det(\boldsymbol{F}) \cdot \widehat{\boldsymbol{T}}_S \cdot \boldsymbol{F}^{T,-1}. \tag{17}$$

Formally, one could notate the fix-point iteration of the FSI for one time-step for fluid and solid solver as nonlinear mappings F and G, respectively, i.e. as

$$\left(\boldsymbol{u}_{k+1}^{n+1}, p_{k+1}^{n+1}\right) = F\left(\boldsymbol{u}_k^{n+1}, p_k^{n+1}, \boldsymbol{w}^{n+1}, \dot{\boldsymbol{w}}^{n+1}\right), \tag{18}$$

$$\left(\boldsymbol{w}_{k+1}^{n+1}, \dot{\boldsymbol{w}}_{k+1}^{n+1}\right) = G\left(\boldsymbol{u}^{n+1}, p^{n+1}, \boldsymbol{w}_k^{n+1}, \dot{\boldsymbol{w}}_k{}^{n+1}\right), \tag{19}$$

with temporal index $n+1$ and iteration index k. In this notation, all constant properties, such as the actual/known values at time index n, are hidden inside functions F and G. By inserting the solution, i.e. the fix-point of the iteration procedure (18-19), one obtains the form

$$F\left(\boldsymbol{u}^{n+1}, p^{n+1}, \boldsymbol{w}^{n+1}, \dot{\boldsymbol{w}}^{n+1}\right) - \left(\boldsymbol{u}^{n+1}, p^{n+1}\right) = 0, \tag{20}$$

$$G\left(\boldsymbol{u}^{n+1}, p^{n+1}, \boldsymbol{w}^{n+1}, \dot{\boldsymbol{w}}^{n+1}\right) - \left(\boldsymbol{w}^{n+1}, \dot{\boldsymbol{w}}^{n+1}\right) = 0, \tag{21}$$

which could be solved by a Newton iteration.

Current work in progress:
We are currently working on three-phase contact line systems with smooth, rigid surfaces. This includes simple contact line models, which use a static contact angle, but will also be extended to more advanced models which support contact angle hysteresis.
This work is expected to be completed by the start of the Priority Programme. Furthermore, ongoing work investigates droplet collisions and merging, as well as ligament breakup.

Work packages:

WP1: Implementation of a second level-set
The first step in this project is the implementation of a second level-set φ_2, which is capable of interacting with the first one, i.e. the implementation of cut cells with two level sets. In this early work package, the following simplifications are proposed:

- The geometry of the deformable solid can be described as a height field $h(t,\xi,\eta)$ with respect to some (potentially curved) solid surface, which is parameterized in coordinates ξ and η.
- For the development, in this very first step, an artificial displacement $h(t,\xi,\eta)$ is prescribed. This can be converted into an explicit Level-Set formulation.

As already noted, the BoSSS code is already capable of tracking more than two fluid phases. It can handle up to four different level-sets and phases can be defined for arbitrary combinations of level-set signs (e.g., assume phases A, B and C, then it can be defined that the negative domain of the first level-set is entirely covered by A, while in the positive region the second level-set discriminates B from C). However, the code still lacks the capability of numerical integration in cells cut by multiple level-sets.
Since it is not known how the HMF procedure can be extended towards multiple level-sets, in a first step we intend to construct volume rules by adaptive subdivision of cells. Such an approach is already implemented in BoSSS [E1] and straightforward to be extended for multiple level-sets. In cells cut by only one level-set still the more efficient HMF will be used.

WP2: Optimized quadrature for cut cells with multiple level-sets
Numerical integration which is based on subdivision, as suggested in the previous WP, is either inaccurate or expensive. It may be sufficient for a “first shot”, but for extensive production runs, a more efficient technique is highly desirable.
We will restrict ourselves to hexahedral background cells; therefore, Saye [27] provided an algorithm based on recursive subdivision: some cell is subdivided until the fluid interface can be described as a graph/height function in each respective subdivision.
Considering two level-sets, we will extend Sayes original algorithm; given two interfaces one encounters situation were one has to describe the area of interest as being bound by two height functions, i.e. by an upper and a lower limit, as e.g. shown in **Figure 7**.

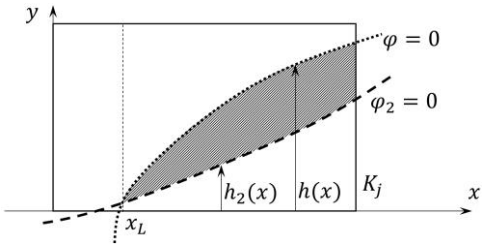

Figure 7: *An integration domain given as the intersection of level-sets from φ and φ_2 (gray area), can be described, after detection of the intersection at x_L be described as the area between two graphs of the height functions h and h_2.*

Since the resulting quadrature method is based on Gaussian rules, it is guaranteed that the accuracy of the flow solver is not compromised by the numerical integration.

WP3: Geometry modeling by 1D Hooks law

A preparation step towards a fully coupled fluid/solid solver is the representation of the geometry by a simplified model, where e.g. each post of a structured surface is modeled as a one-dimensional spring, as shown in **Figure 8**. In such an approach, even a change of the solid volume may be acceptable.

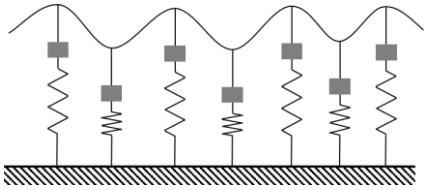

Figure 8: *In a simplified setup, the flexible interface may be described as a spline, where the individual control knots are defined by mass/spring/damper systems.*

Apart from being easier to simulate, this approach also allows to study the first-order qualitative principles instead of an entire system with compound (and sometimes rivaling) effects, e.g. shear components in the solid are neglected.

WP4: Coupling with external structural solver

In order to verify the first-order principles found in [WP3], fully coupled simulations, which also incorporate coupling to a solid structure solver that supports linear elastic materials such as silicon rubber, will be performed. We intend to use some pre-existing, 3rd party toolbox (COMSOL) instead of developing a separate solver.

The main advantage of this approach is that the time required for code development can be shortened and thus the cooperation work packages can be started at an early stage.

This work package can be broken down into three sub-packages:

- technical coupling: This concerns the software-technical “hook-up” of two different software packages. The structural solver has to be integrated into the larger FSI framework, therefore an appropriate software interface for data exchange and control of the solver (e.g. time-stepping) is required. Since BoSSS is implemented in C#, resp. the .NET framework, a bridging technology may be required. COMSOL can be controlled via a Java application program interface (API). The specific parts of this API that are required to realize the intended coupling could be wrapped in a dynamic library with C-functions in order to be callable from C#. In subsequence, the data obtained from COMSOL has to be interpolated on a BoSSS mesh.
- Implementation of the displacement-controlled second interface $\mathcal{J}_2(t)$, as described above.
- Implementation and Testing of the FSI loop: as described above, we first aim for the implementation of a loose coupling and in subsequence evolve this into a strong coupling. Both will be tested using generic FSI benchmarks.

WP5: Pinning of level-sets at edges of printing shapes

In order to realize the setup “Flexible roller”, see **Figure 5**, it is required to implement a pinning functionality for the liquid/gas level-set φ, in order to reproduce the pinning effect of the edge of the liquid film at the edged of the printing plate elevations.

This can be achieved by adding a diffusion term into the level-set equation (11), i.e. by the modified level-set equation

$$\partial_t \varphi + \nabla\varphi \cdot \boldsymbol{u} = \mathrm{div}(\varepsilon(\boldsymbol{x})\, \nabla\varphi). \tag{22}$$

The local diffusion parameter $\varepsilon(\boldsymbol{x})$ is chosen to be nonzero only in a small region of diameter w around the pinning edge, e.g.

$$\varepsilon(\boldsymbol{x}) = \begin{cases} \frac{w^2}{w^2+\delta(\boldsymbol{x})^2}, & |\delta(\boldsymbol{x})| < w \\ 0, & |\delta(\boldsymbol{x})| \geq w \end{cases}, \tag{23}$$

where $\delta(\boldsymbol{x})$ denotes the shortest distance between $\boldsymbol{x}$ and the pinning edge. This additional second order term allows, resp. requires a Dirichlet boundary condition for φ in regions where $\varepsilon(\boldsymbol{x})$ is nonzero. By including the zero-crossing in the boundary condition, the interface $\mathcal{J}$ remains pinned at the respective location.

C-WP1: Cooperation work Package: elementary experiments

In cooperation with the Project of K. Harth (University of Twente) we agreed on the simulation of the setups “Liquid Bridge” and “Droplet Impact” shown in **Figure 3** and **Figure 4**.

These setups certainly represent laminar flow configurations. Therefore it is possible to start with 2D simulations and proceed to 3D setups.

The Liquid Bridge experiment is supposed to be easier to control, since no topology changes occur. It is also a very important numerical validation test case to determine whether the deformation of the flexible substrate, as well as the position and current contact angle are correctly predicted. Beside the plate movement, the thickness of the substrate will be varied in the range of 10 µm to 1 mm.

Therefore, the cooperation partner will provide values for the advancing and the receding contact angle, as well as material parameters for the flexible substrate.

As already noted above, in the Droplet Impact experiment, the physical mechanism which triggers, resp. initiates the wetting is not very well understood and therefore, but also due to length scale issues, cannot be represented in the numerical simulation. Hence, the topology change will be the result of a numerical artifact. By a series of parameter studies we strive to identify parameter areas in which the simulation nevertheless provides physically correct results.

In order to correctly reproduce the ligament breakup as well as droplet contact, an appropriate **feature-based indicator for adaptive mesh refinement** has to be developed.

C-WP2: Cooperation work package: Printing applications

In cooperation with the Project of E. Dörsam (Printing Science Technology, TU Darmstadt) we agreed on the simulation of the setups “Flexible Roller” and “Flexible Substrate” shown in **Figure 5** and **Figure 6**.

In the numerical representation, the fluid interface between air and ink is represented by level set φ, while the boundary of the soft layer is represented by the second level set φ_2. In both setups, hard surfaces can be modeled as a Dirichlet boundary condition with a tangential velocity (“moving wall” boundary condition). A simulation domain as shown in **Figure 9** will be used.

In the realistic experiment, the following dimensions can be found:

- radius of the roller: 10 cm
- thickness of ink film: 15 µm
- wetted length (size of structure to print): 100 µm to 1 mm
- minimal nip width: 1 µm
- printing velocity v_P: up to 5 m/sec at IDD’s facilities

It is further known, from practical applications of flexographic printing that the main curvature of the fluid meniscus at the outgoing nip is subject to strong variations: while being about as small as 1 µm in radial direction, it can be up to 1 mm in axial direction.

The work package is divided into **two phases**; in the first phase (“**ramp up**”), the problem size and simulation complexity are increased step-by-step, until the simulation of the full setup for both setups is established. In the second phase (“**production runs**”), the physical-technical investigations are to be carried out, which includes e.g. parameter variations.

In the ramp-up phase, the complexity of the simulation will be increased in three steps:

1. Simulation **without FSI**, i.e. rollers and substrate are assumed to be rigid
2. **Simplified FSI** using mass/spring/damper systems, as described in WP3
3. **Full FSI**, as described in WP4, WP5

Furthermore, all of these setup will first be simulated in **2D before full 3D** simulations are carried out. Due to the strong variation of length scales, i.e. between the minimal length of the nip and the wetting length or within the fluid interface, an appropriate **feature-based indicator for adaptive mesh refinement** has to be developed.

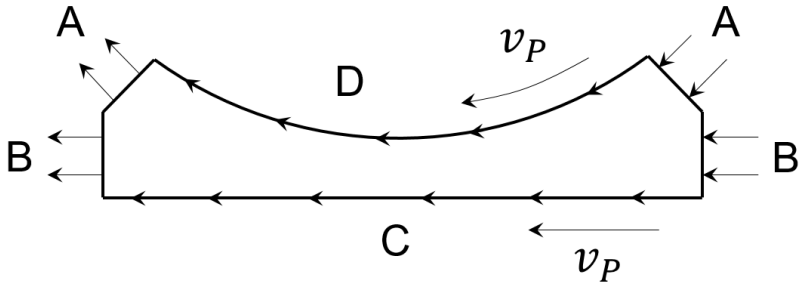

Figure 9: Simulation domain for the "Flexible Roller" and "Flexible Substrate" setups. Periodic boundary conditions are used for boundaries A and B. Both, the upper wall D as well as the lower wall C move tangential with printing velocity v_P. For the flexible roller setup, the wall D is the boundary between flexible solid and fluid, i.e. the interface $\mathcal{J}_2$, which is the zero-level-set of the field $\varphi_2(t,\boldsymbol{x})$, while wall C is a solid wall with tangential velocity. For the Flexible Substrate setup, the roles of C and D are exactly reversed. In span-wise direction, for 3D simulations, periodic boundary conditions are assumed.

For the production runs, at first an appropriate post-processing routine has to be developed which is capable of extracting the integral measures described in the objectives, e.g. to compute the statistical distribution of wavelengths for the contact line shape at the outgoing nip.
Regarding the parameter studies, the main benefit of simulations is to variate parameters that are difficult or expensive to change in the physical experiment, e.g. viscosity values of the ink or material constants for the flexible substrate. Parameters, resp. parameter ranges will be provided by the cooperation partner.
Depending on the scale and number of the simulations to perform, either Institute-owned facilities or the Lichtenberg high-performance-computing system (see also section 5.5) will be used.

Schedule

	2019	2020				2021				2022		
	Q4	Q1	Q2	Q3	Q4	Q1	Q2	Q3	Q4	Q1	Q2	Q3
WP1	X	X	X									
WP2		X	X	X								
WP3			X	X	X							
WP4				X	X	X	X	X				
WP5									X			
cWP1				X	X	X	X	X	X	X	X	X
cWP2				X	X	X	X	X	X	X	X	X

Continuation of Project in the second period:
The overall goal for the continuation of the project in the second funding period is to develop the numerical framework which is set up here to capture more physical effects. One objective would e.g. be to verify PDE-based models for novel materials (e.g. coatings based on polymer brushes) in a larger setup.
Standard examples are the treatment of surfactant transport equations, which is a research area that has already been addressed with the BoSSS code as part of the Priority Programme 1506, "Transport Processes at Fluidic Interfaces".
Another possibility is the simulation of systems with more than two fluid phases, e.g. to numerically predict the wetting behavior of liquid infused surfaces.

2.4 Data handling

Source Code:
The most important data produced by this project certainly is the source code itself. Since its early beginnings, the code development of BoSSS was tracked using the Git[1] version control system. The BoSSS code itself is already publicly available on Github[2].

Simulation results:
Simulation results are saved on servers with backup within our institute in two file formats, the BoSSS-native one as well as Tecplot. The former one is database-centric, i.e. simulation results are stored together with additional information like application settings, etc..
Simulation Results which are part of a publication will be stored

- internally, on the institute-owned file servers
- publically, on the "simpleArchive"[3] platform which is provided by TU Darmstadt free of charge for data amounts up to 1 TB. "simpleArchive" provides permanent URL's for registered data which can be included in publications.

Reproduction of simulation results:
The reproducibility of calculations with BoSSS is based on two components: Firstly, the script control implemented allows a specific calculation, including pre- and post-processing, to be repeated, on demand, at any time. Second, the version control system Git allows to restore any arbitrary version of the code.
This setup allows us or others to reproduce any specific, publication-relevant computation and the relevant statistics. The respective scripts are also stored in the Git repository. By using a continuous integration build process, the maintenance of these scripts is assured.

2.5 Other information

2.6 Descriptions of proposed investigations involving experiments on humans, human materials or animals as well as dual use research of concern

Not applicable

2.7 Information on scientific and financial involvement of international cooperation partners

Not applicable

2.8 Information on scientific cooperation within SPP

- *K. Harth, University of Twente:* The contents of the cooperation are outlined in work package C-WP1. At the present time, K. Harth works as a Postdoctoral Researcher at the University of Twente; She plans to take up a position in Germany before the anticipated start of the priority programme.
- *E. Dörsam, TU Darmstadt, Institute of Printing Science and Technology (IDD):* The contents of the cooperation are outlined in work package C-WP2. In addition to already existing cooperation meetings in the Collaborative Research Centre 1194, regular working meetings of the financed employees are planned. Due to the proximity of the institute's locations, meetings can be scheduled at short notice.
- *A. Reusken, Chair for Numerical Mathematics, RWTH Aachen:* In the joint project of A. Reusken and S. Hardt (Institute for Nano- and Microfluidics, TU Darmstadt) XFEM methods for the simulation of water droplets on thin silicone oil layers are applied; numerical research is carried out at the institute of A. Reusken, while S. Hardt works on

[1] https://git-scm.com/
[2] https://github.com/FDYdarmstadt/BoSSS
[3] https://www.hrz.tu-darmstadt.de/speicherplatz_datensicherung_und_server/simplearchive_hrz/index.en.jsp

experiments and theoretical modelling. Due to the similarity of the numerical approaches, we agreed on regular exchange on numerical issues of extended Galerkin formulations: this includes e.g. the variational formulation of contact line models, preconditioning of linear solvers and general stabilization techniques.

- *S. Aland, Faculty of Informatics / Mathematics, HTW Dresden:* In S. Aland's project, a phase-field method is used to simulate wetting of flexible substrates. Although the numerical methods are different, the objectives are similar. It was agreed to perform both qualitative and quantitative comparisons of both numerical methods.

3 Bibliography

[1] W. H. Reed and T. R. Hill, "Triangular mesh methods for the neutron transport equation," in *National topical meeting on mathematical models and computational techniques for analysis of nuclear systems*, 1973, p. 23.

[2] B. Cockburn and C.-W. Shu, "The P1-RKDG Method for Two-dimensional Euler Equations of Gas Dynamics," 1991.

[3] D. N. Arnold, "An Interior Penalty Finite Element Method with Discontinuous Elements," *SIAM J. Numer. Anal.*, vol. 19, no. 4, p. 742, 1982.

[4] I. Babuška, "The finite element method for elliptic equations with discontinuous coefficients," *Computing*, vol. 5, no. 3, pp. 207–213, Sep. 1970.

[5] J. W. Barrett and C. M. Elliott, "Fitted and Unfitted Finite-Element Methods for Elliptic Equations with Smooth Interfaces," *IMA J. Numer. Anal.*, vol. 7, no. 3, pp. 283–300, 1987.

[6] N. Moës, J. Dolbow, and T. Belytschko, "A finite element method for crack growth without remeshing," *Int. J. Numer. Methods Eng.*, vol. 46, pp. 131–150, Sep. 1999.

[7] J. Chessa and T. Belytschko, "Arbitrary discontinuities in space-time finite elements by level sets and X-FEM," *Int. J. Numer. Methods Eng.*, vol. 61, no. 15, pp. 2595–2614, Dec. 2004.

[8] S. Groß and A. Reusken, "An extended pressure finite element space for two-phase incompressible flows with surface tension," *J. Comput. Phys.*, vol. 224, no. 1, pp. 40–58, May 2007.

[9] S. Groß and A. Reusken, "Finite Element Discretization Error Analysis of a Surface Tension Force in Two-Phase Incompressible Flows," *SIAM J. Numer. Anal.*, vol. 45, no. 4, pp. 1679–1700, Jan. 2007.

[10] T. P. Fries, "The intrinsic XFEM for two-fluid flows," *Int. J. Numer. Methods Fluids*, vol. 60, no. 4, pp. 437–471, Jun. 2009.

[11] K.-W. Cheng and T.-P. Fries, "XFEM with hanging nodes for two-phase incompressible flow," *Comput. Methods Appl. Mech. Eng.*, vol. 245–246, pp. 290–312, Oct. 2012.

[12] H. Sauerland and T.-P. Fries, "The stable XFEM for two-phase flows," *Comput. Fluids*, vol. 87, pp. 41–49, Oct. 2013.

[13] P. Bastian and C. Engwer, "An unfitted finite element method using discontinuous Galerkin," *Int. J. Numer. Methods Eng.*, vol. 79, no. 12, pp. 1557–1576, Sep. 2009.

[14] F. Heimann, "An Unfitted Higher-Order Discontinuous Galerkin Method for Incompressible Two-Phase Flow with Moving Contact Lines," PhD thesis, Heidelberg University, Heidelberg, 2013.

[15] P. Causin, J. F. Gerbeau, and F. Nobile, "Added-mass effect in the design of partitioned algorithms for fluid–structure problems," *Comput. Methods Appl. Mech. Eng.*, vol. 194, no. 42–44, pp. 4506–4527, Oct. 2005.

[16] M. Lukáčová-Medvid'ová, G. Rusnáková, and A. Hundertmark-Zaušková, "Kinematic splitting algorithm for fluid–structure interaction in hemodynamics," *Comput. Methods Appl. Mech. Eng.*, vol. 265, pp. 83–106, Oct. 2013.

[17] Y. Bazilevs, V. M. Calo, Y. Zhang, and T. J. R. Hughes, "Isogeometric Fluid–structure Interaction Analysis with Applications to Arterial Blood Flow," *Comput. Mech.*, vol. 38, no. 4–5, pp. 310–322, Sep. 2006.

[18] H. Beirão da Veiga, "On the Existence of Strong Solutions to a Coupled Fluid-Structure Evolution Problem," *J. Math. Fluid Mech.*, vol. 6, no. 1, pp. 21–52, Mar. 2004.

[19] H. G. Matthies and J. Steindorf, "How to make weak couplings strong," in *Computational Fluid and Solid Mechanics*, Amsterdam, 2001.

[20] H. G. Matthies and J. Steindorf, “Partitioned strong coupling algorithms for fluid–structure interaction,” *Comput. Struct.*, vol. 81, no. 8–11, pp. 805–812, May 2003.
[21] F. Alauzet, B. Fabrèges, M. A. Fernández, and M. Landajuela, “Nitsche-XFEM for the coupling of an incompressible fluid with immersed thin-walled structures,” *Comput. Methods Appl. Mech. Eng.*, vol. 301, pp. 300–335, Apr. 2016.
[22] P. F. Antonietti, M. Verani, C. Vergara, and S. Zonca, “Numerical solution of fluid-structure interaction problems by means of a high order Discontinuous Galerkin method on polygonal grids,” MOX-Report, Politecnico di Milano, Milano, 27/2018, 2018.
[23] J. E. Sprittles and Y. D. Shikhmurzaev, “Finite element framework for describing dynamic wetting phenomena,” *Int. J. Numer. Methods Fluids*, vol. 68, no. 10, pp. 1257–1298, Apr. 2012.
[24] D. Legendre and M. Maglio, “Comparison between numerical models for the simulation of moving contact lines,” *Comput. Fluids*, vol. 113, pp. 2–13, May 2015.
[25] A. Karakus, T. Warburton, M. H. Aksel, and C. Sert, “A GPU-accelerated adaptive discontinuous Galerkin method for level set equation,” *Int. J. Comput. Fluid Dyn.*, vol. 30, no. 1, pp. 56–68, Jan. 2016.
[26] S. Ganz *et al.*, “Printing and Processing Techniques,” in *Organic and Printed Electronics: Fundamentals and Applications*, New York: Taylor & Francis, 2016, pp. 47–116.
[27] R. I. Saye, “High-Order Quadrature Methods for Implicitly Defined Surfaces and Volumes in Hyperrectangles,” *SIAM J. Sci. Comput.*, vol. 37, no. 2, pp. A993–A1019, Jan. 2015.

4 Requested modules/funds

4.1 Basic Module

4.1.1 Funding for Staff

Research staff: The tasks are intended to be conducted by a PhD candidate; According to a communication by the Priority Programme Coordinator, only 75% of the PhD position should be funded through Priority Programme funds. However, the work programme of this project requires a full-time involvement in the project. In addition, doctoral positions in mechanical engineering at the TU Darmstadt are usually full-time positions and it is typically difficult to attract excellent candidates for a 75% position. Therefore we kindly request the financing of a 100% position.
Member of the scientific staff: **TV-H E13 for 36 months**

Student research assistant: A part of the required implementation and verification tasks will have to be performed by student research assistants.
Student research assistant from the second year: 80 h/month for 36 months
At TU Darmstadt the hourly rate for a student assistant is 11.50 e. In consideration of the additionalsocial costs it amounts to about 16.50 € / h.
Total costs for the student research assistant:

80 h/month × 36 months × €16.50 / hour = € 47 520

4.1.2 Direct Project Costs

4.1.2.1 Equipment up to Euro 10,000, Software and Consumables

Funding is requested for the supply of data processing consumables (CD, DVD, paper, toner, etc.).

Sum for three years: € 1 000

4.1.2.2 Travel Expenses

In order to provide the embedding into general Priority Programme, a series of events are planned:

- 1st, 2nd year: workshop (4 days) where employed researcher and PI participate
- 1st year: advanced school (5 days) for employed researcher

- 2nd year: Phd-candidate workshop (4 days) for employed researcher
- 3rd year: international conference (5 days) where employed researcher and PI contribute

According to guidelines specified by the Priority Programme Coordinator, we assume € 200 for traveling expenses and additional € 80 per person per day for accommodation.

Sum overall: € 4 400

Additionally, we request for traveling funds for the PhD candidate to participate in another international conference which is not organized as part of the Priority Programme (conference fee, traveling expenses and accommodation)

Sum overall: € 3 000

4.1.2.3 Visiting Researchers (excluding Mercator Fellows) none
4.1.2.4 Expenses for Laboratory Animals not applicable
4.1.2.5 Other Costs none

4.1.2.6 Project-related publication expenses

We intend to publish all publications as open-access. The current fees for a typical journal, i.e. the Journal of Computational Physics (JCP) are 2 600 USD. However, the DFG grants a maximum support of € 750 per year.

Sum for three years: € 2 250

4.1.3 Instrumentation

4.1.3.1 Equipment exceeding Euro 10,000 none
4.1.3.2 Major Instrumentation exceeding Euro 50,000 none

4.2 Module Temporary Position for Principle Investigator not applicable
4.3 Module Replacement Funding not applicable
4.4 Module Temporary Clinician Substitute not applicable
4.5 Module Mercator Fellows none
4.6 Module Workshop Funding none
4.7 Module Public Relations Funding none

5 Project requirements

5.1 Employment status information

- **Kummer, Florian, Dr.-Ing.:** permanent position, state funding.

5.2 First-time proposal data

not applicable

5.3 Composition of the project group

- **Kummer, Florian, Dr.-Ing.:** permanent position, state funding. Research group leader and project PI, initiator and main developer of the BoSSS code, who will provide technical support as well support for project-critical implementation tasks.
- **Oberlack, Martin, Prof. Dr.-Ing. habil.:** permanent position, state funding. Supporting and co- supervising the project in his capacity as head of the Chair of Fluid Dynamics.
- **Wang, Yongqi, Prof. Dr.-Ing. habil.:** permanent position, state funding. Supporting and co- supervising the project in his capacity as deputy of the Chair of Fluid Dynamics.

5.4 Cooperation with other researchers

5.4.1 Researchers with whom you have agreed to cooperate on this project

see section: **2.8 - Information on scientific cooperation within SPP**

5.4.2 Researchers with whom you have collaborated scientifically within the past three years

- Warburton, Tim Prof. Virginia Tech USA
- Egger, Herbert Prof. Dr. TU Darmstadt Germany
- Lukácová-Medvidová, Mária Prof. Dr. JGU Mainz Germany
- Speck, Thomas Prof. Dr. JGU Mainz Germany
- Virnau, Peter Prof. Dr. JGU Mainz Germany
- Members of the Collaborative Research Centre 1194[4]
- Members of the Collaborative Research Centre 146[5]

5.5 Scientific equipment

Lichtenberg-Supercomputer:
The TU Darmstadt hosts the so-called “Lichtenberg” supercomputer which has been funded by the German Research Foundation. Lichtenberg was installed in two phases. The first phase has been installed in 2013, the second phase was installed 2015. Overall the hardware of the two phases consist of about 1400 nodes[6].
The planning of a successor system, "Lichtenberg-2", which is scheduled to enter production operation in Q4/2019, is currently underway at the TU Darmstadt.
For members of the TU Darmstadt, computing times are granted via an internal application and evaluation procedure.

5.6 Project-relevant cooperation with commercial enterprises none

5.7 Project-relevant participation in commercial enterprises none

6 Additional information

none

[4] https://www.sfb1194.tu-darmstadt.de/sfb_1194/kontakt_9/index.en.jsp
[5] https://trr146.de/
[6] http://www.hhlr.tu-darmstadt.de/hhlr/index.en.jsp